Nuclear Instruments and Methods in Physics Research B59/60 (1991) 772–777
North-Holland

Improvement of corrosion resistance of M50 bearing steel by implantation with metal ions *

B.R. Nielsen and B. Torp
Danfysik A/S, DK-4040 Jyllinge, Denmark

C.M. Rangel, M.H. Simplicio and A.C. Consiglieri
Dept. of Materials Technology, LNETI, P-1699 Lisboa, Portugal

M.F. DaSilva and F. Paszti
Dept. of Physics, LNETI, P-2685 Sacavem, Portugal

J.C. Soares
Centre of Nuclear Physics, University of Lisbon, P-1699 Lisboa, Portugal

A. Dodd and J. Kinder
Bearings Research Centre, RHP Bearings Ltd., Newark NG24 2JF, England, UK

M. Pitaval and P. Thevenard
Dept. of Physics, Université de Claude Bernard, F-69622 Villeurbanne, France

R.G. Wing
Materials Laboratory L2, Rolls Royce PLC, Watford WD2 7BZ, England, UK

With the overall objective to improve the service life and reliability of gas turbine engine bearings by increasing their corrosion resistance and rolling contact fatigue life a collaborative project under the EEC BRITE/EURAM programme has been initiated. The project is aimed at developing an ion implantation technique to implant bearing components with metallic species and to optimise the process particularly for applications where salt-water contamination of the lubricating oil might occur. Prior to implanting into bearing components, test specimens of M50 bearing steel implanted with Cr^+ and Ta^+ at several doses have been characterised by various techniques. This article reports on the implantation work, the RBS and NRA analysis for depth profiling and independent dose measurement, and the corrosion resistance measurements which have been performed in order to determine the optimum treatment.

1. Introduction

The service life of gas turbine engine bearings is often limited by corrosion, which causes excessive wear of the bearing components. It has been proven that even minor corrosion pitting of the bearing raceways reduces life considerably. The corrosion problems are particularly important in situations where a risk of salt-water contamination of the lubricating oil exists, such as in carrier-based aircrafts and helicopters in service at oil rigs. The fact that up to 80% of the bearings are removed from service due to corrosion problems emphasises the importance of improving corrosion resistance of these parts for safety reasons as well as from economical considerations.

With the overall objective to improve the service life and reliability of gas turbine engine bearings by increasing their corrosion resistance and rolling contact fatigue

* This project is funded by the EEC under BRITE/EURAM contract no. RI1B-284.

0168-583X/91/$03.50 © 1991 – Elsevier Science Publishers B.V. (North-Holland)

life, a collaborative project under the EEC BRITE/EURAM programme has been initiated. The project is aimed at developing an ion implantation technique to implant bearing components with metallic species and to optimise the process particularly for applications where salt-water contamination of the lubricating oil may occur.

The project flow follows a systematic route of investigation from implantation into simple coupon specimens to final testing of real gas turbine engine bearings under severe corrosion and wear conditions. The roles of the individual partners of the project are to perform the tasks whithin their field of expertise.

Simple coupon samples of M50, T1, M50NiL (carburized and uncarburized) will be implanted with various ion species, doses, and angles of incidence. The samples will be used in corrosion tests, except for a few which will be analysed by ion beam analysis techniques to investigate the depth profiles and retained doses, thus enabling quantification of all implants made throughout the whole programme. Polymet specimens in the various bearing steels will be implanted with the same species and doses as for the coupons and used for rolling contact fatigue test to determine the optimum proces parameters for maximum fatigue life [1]. The above tests will be further complemented by Auger analysis and scanning electron microscopy.

When optimum implantation parameters have been established, two types of bearings (type 7208 and 7305) in M50 steel will be implanted and subsequently tested to assess the life of bearings at elevated temperatures typical of gas turbine engines and in contaminated lubricant.

Finally, implanted Rolls Royce GEM engine bearings will be tested under conditions representative of the maximum operating conditions of an aero-engine in both clean and contaminated oils and then subjected to high humidity to determine the effectiveness of the implantation.

The present article describes the work performed so far and the results obtained from chromium and tantalum implanted M50 steel.

2. Implantations

The ion implantations were performed on a Danfysik Series 1090 high current implanter, which is a 200 keV universal implanter with mass analysis and "all magnetic" beam transport designed specifically for IBMM processes. The implanter is described in detail elsewhere [2].

A new electromagnetic beam scanning system was designed in order to be able to implant large batches of balls and bearing raceways. The system consists of two laminated dipole magnets with water-cooled coils, one magnet for the horizontal sweep and one for the vertical sweep. The possible scanning area is dependent on the mass and energy of the ions, e.g. 200 keV tantalum can be scanned 35 cm by 35 cm and 200 keV chromium can be scanned 40 cm by 40 cm, which is the mechanical limit due to the design of the target chamber.

Fig. 1. The general-purpose water-cooled sample manipulator with coupon samples mounted.

The general-purpose sample manipulator of the implanter as shown in fig. 1 was used for mounting the samples in the implantation chamber. It has three independent movements, a rotation, a linear motion and a tilt. The target is directly water cooled. The manipulator is designed so that special target holders can be mounted, e.g. for ball implantations and implantation of bearing raceways.

The implanter was upgraded with cryopumps in the beam line and in the target chamber to ensure an oil-free vacuum. The base vacuum is 1×10^{-6} mbar increasing to between 2 and 5×10^{-6} mbar during implantation.

The ion species selected for this study were Cr^+ and Ta^+. The coupons were implanted with 180 keV Cr^+ ions in doses of 0.5, 1.0, 2.0, and 4.0×10^{17} at./cm^2, while 180 keV Ta^+ doses were limited to 5×10^{16} at./cm^2, since higher retained doses cannot be achieved due to the high sputter yield [3].

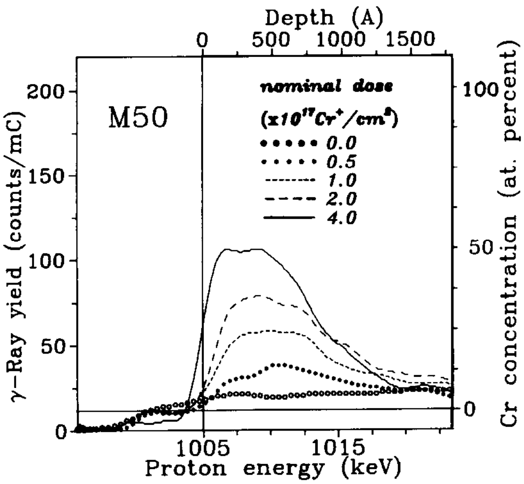

Fig. 2. The chromium profile as a function of depth in M50 steel for different 180 keV Cr^+ implantation doses.

The sample temperature was continuously monitored by an infrared detector during the implantations and was kept below 250 °C.

3. Depth profiles

The Cr^+ implantations were studied using the (p, γ) resonance broadening method with the $^{52}Cr(p, \gamma)^{53}Mn$ nuclear reaction at $E_p = 1005$ keV [4,5]. The gamma rays were detected with a 3 × 3 NaI(Tl) detector at an angle of 0° with respect to the proton beam and at a distance of 1 cm from the target placed perpendicular to the beam. From the measured Cr depth profile the concentrations and the retained doses were calculated. A pure Cr sample (99.9%) measured under similar experimental conditions was used for calibration of the absolute Cr content.

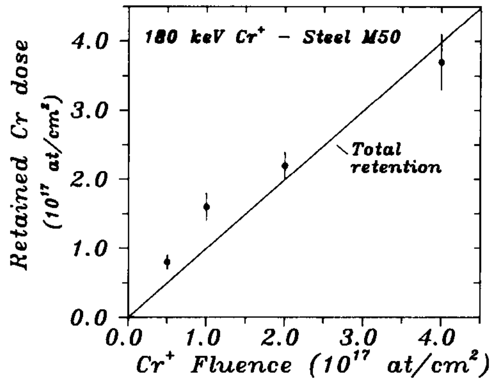

Fig. 3. The retained dose as a function of the implanted dose for chromium into M50 steel.

The profiles for Cr implantation into M50 are shown in fig. 2. The "background level" for the unimplanted sample is due to the Cr content in the M50 steel. In fig. 3 the nominal dose (measured during implantation) is compared with that obtained from the ion beam analysis for Cr into M50 steel. Taking into account an estimated 25% uncertainty on the nominal dose measurement we observe a reasonable agreement between the nominal and measured doses, although the trend of

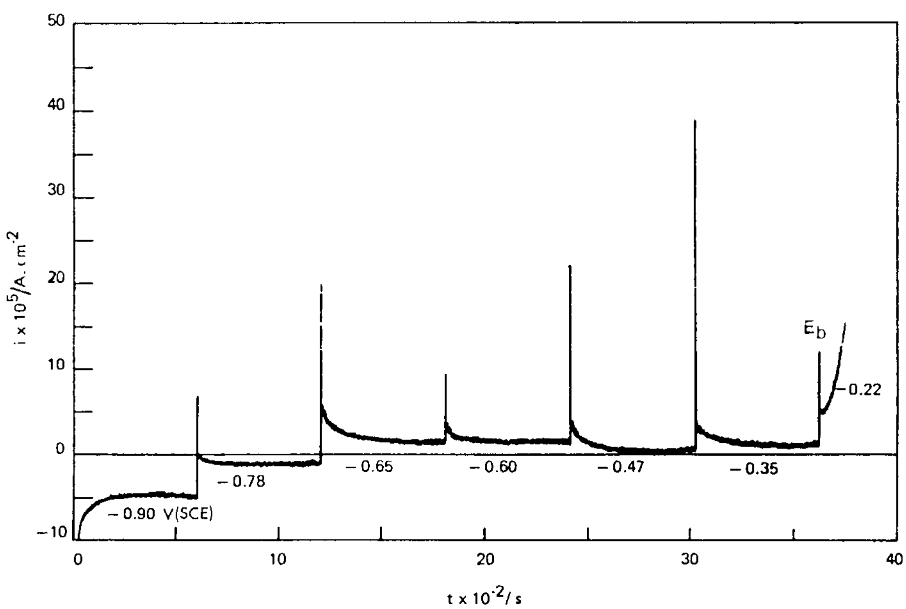

Fig. 4. Step-by-step potentiostatic polarisation for M50 steel in 0.5M $NaHCO_3$ + 0.05M Na_2CO_3 + 0.5M NaCl solution. The current density vs time plot indicates breakdown potential at −220 mV (SCE).

the data indicates a reduced retained dose at the 4×10^{17} at./cm^2 level which is due to sputtering (sputtering yield, $Y \approx 4.4$ atoms/ion).

The implanted Ta was depth profiled using Rutherford back-scattering spectrometry (RBS) [6]. The energy of the He^+ beam was 1.6 MeV and the backscattered particles were detected at 140° relative to the incident beam with a silicon surface barrier detector. The retained dose as measured from the depth profiles was in agreement with the nominal dose at 5×10^{16} at./cm^2, while a few samples implanted with higher doses (up to 4×10^{17} at./cm^2) showed that the maximum retained dose for 180 keV Ta^+ is $\approx 5 \times 10^{16}$ at./cm^2 (sputtering yield ≈ 15.4 atoms/ion).

4. Corrosion behaviour

The corrosive properties of implanted and unimplanted M50 steel coupons were electrochemically characterized using cyclic voltammetry in carbonate/bicarbonate solutions with added chloride ions at room temperature and at several scan rates.

In the case of unimplanted samples three anodic peaks were observed in agreement with published literature [7,8] together with a wide reduction peak. Analysis of peak currents indicates possible diffusion control of the anodic process [9]. The breakdown potentials (E_b) were estimated to be between −225 and −240 mV (SCE) depending, as expected, on sweep rate.

Potentiostatic testing indicated E_b values in the neighbourhood of −220 mV in agreement with potentiodynamic values. In fig. 4 is shown the M50 steel current density vs time profile resulting from step-wise polarization departing from a cathodic limit of −0.90 V (SCE).

The effect of Cr^+ implantation on the polarization characteristics of M50 steel is illustrated in fig. 5, where the peak current is shown as a function of the scan rates in a log–log plane. The relationship is found to be

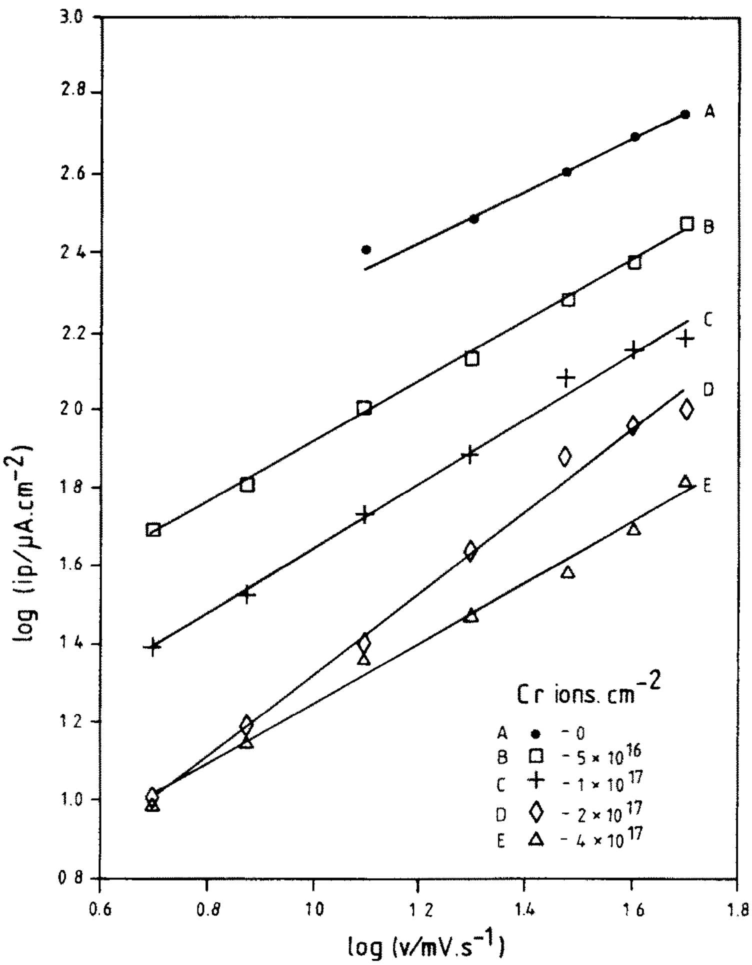

Fig. 5. Polarization characteristics for 180 keV Cr^+ implanted M50 samples and base metal. The peak current density (i_p) is shown as a function of sweep rate (v) for various ion doses.

linear with significant differences between doses in the range from 5×10^{16} to 4×10^{17} at./cm^2 indicating an improvement in corrosion resistance. Even though the 4×10^{17} at./cm^2. Cr-implanted surface gives smaller currents, pitting potential might, as suggested in the figure, be more active than for 2×10^{17} at./cm^2. At this dose the peak current density at 12.5 mV/s scan rate is reduced by a factor ≈ 6.5 relative to the unimplanted samples.

Tantalum, like chromium is known to form highly protective films very readily and was also chosen as a species to be implanted in this programme. For Ta implantation into M50 (fig. 6) we observe a similar decrease in the anodic current density as observed for Cr implantation. At 5×10^{16} at./cm^2 the peak current density is reduced by a factor ≈ 4.5 at 12.5 mV/s scan rate.

The observed increase of the breakdown potential as a result of implantation is remarkable with an increase in E_b of more than 0.5 V (SCE) for both Cr^+ and Ta^+ implanted samples, figures indicating slightly better performance for Cr^+ implantations. For long-term exposure tests in open-circuit conditions the occurrence of crevices was noticeable at the interface between the implanted and nonimplanted surfaces. This behaviour was suggested by fluctuations in the open-circuit potential and confirmed by attack morphology observations on a scanning electron microscope for both Cr and Ta implanted samples. When crevice-free samples were used, results indicated higher open-circuit potential values with differences up to 0.25 V (SCE).

The corrosion behaviour of Fe–Cr surface alloys produced by ion implantation is comparable to that exhibited by Fe–Cr alloys produced by conventional methods [10,11] with improvement in localized corrosion resistance in chloride-containing solutions.

The decrease in the anodic current density of the Ta^+ implanted samples may be explained by the passivating effect produced by the formation of a Ta_2O_5 film during exposure and/or polarization. Breakdown and

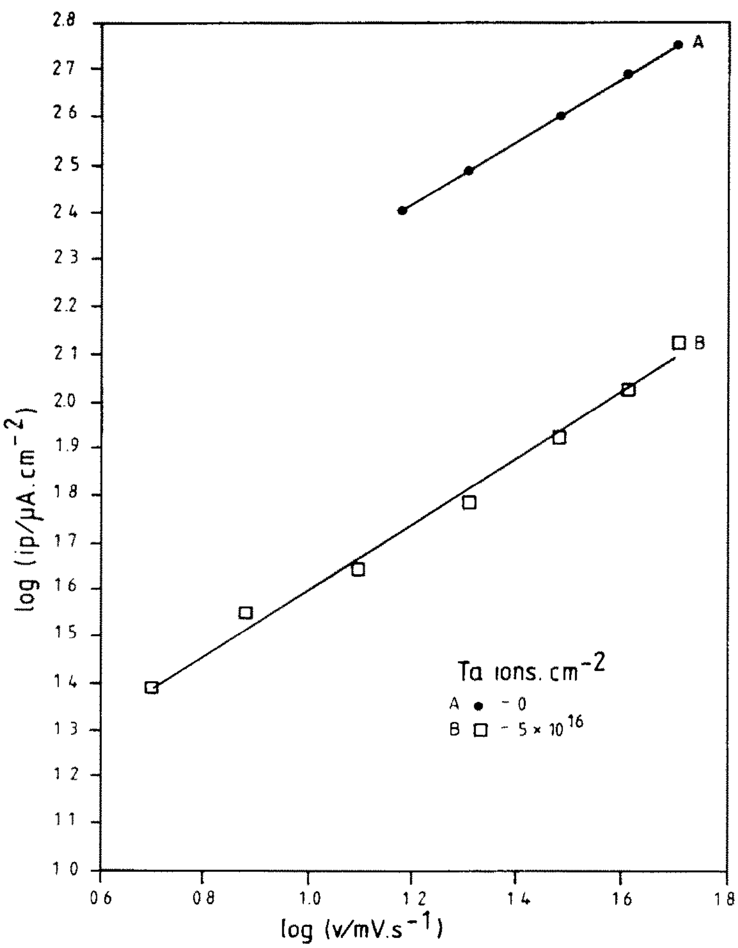

Fig. 6. Polarization characteristics for 180 keV Ta^+ implanted M50 samples and base metal. The peak current density (i_p) is shown as a function of sweep rate (v) for various ion doses.

dissolution of Fe–Ta surface alloy layers is of the localized type with preferential dissolution of iron. This is suggested as a result of EDS (energy dispersive spectrometry) analysis in active and passive adjacent zones in a crevice, where the amount of detected Ta was not significantly different.

Eventually the effect of Ta could be eliminated by extensive anodic dissolution with loss of the implanted material.

5. Conclusions

The test results on implanted specimens obtained so far show that there is a reasonable agreement between the as-implanted Cr^+ doses and the retained doses measured by NRA with some indication of lack of retention due to sputtering at the highest dose. The retained Ta^+ dose measured by RBS analysis shows good agreement with the as-implanted dose at 5×10^{16} at./cm^2. Due to the high sputtering yield of Ta^+ the retained dose is not increased at higher implanted doses.

The implantation of Ta^+ and Cr^+ produced a significant improvement in the corrosion resistance of M50 steel. The polarization characteristics showed a reduction of the peak current density by factors 6.5 and 4.5 for Cr^+ and Ta^+, respectively. Furthermore, an increase of about 0.5 V of breakdown potential was found as a result of implantation of both species.

References

[1] A.T. Galbato in: Rolling Contact Fatigue Testing of Bearing Steels (ASTM, Philadelphia, 1981) p. 169.
[2] B.R. Nielsen, P. Abrahamsen and S. Eriksen, Mater. Sci. Eng. A116 (1989) 193.
[3] V. Ashworth, D. Baxter, W.A. Grant and R.P.M. Procter, Corr. Sci. 17 (1977) 947.
[4] R.L. Schulte, J.D. King and H.W. Taylor, Nucl. Phys. A243 (1975) 202.
[5] M.F. DaSilva, A.A. Melo, K. Freitag and J.C. Soares, Nucl. Instr. and Meth. 209/210 (1983) 889.
[6] W.K. Chu, J.W. Mayer and M.-A. Nicolet, Backscattering Spectrometry (Academic Press, New York, 1978).
[7] C.R. Valentini, C.A. Moine, J.R. Vilche and A.J. Arvia, Corr. Sci. 25 (1985) 985.
[8] C.M. Rangel, R.A. Leitao and I.T. Fonseca, Electrochim. Acta 34 (1989) 355.
[9] C.M. Rangel, M.H. Simplicio and A.C. Consiglieri, Internal Report SCPM/RP/5/90, LNETI (1990).
[10] B.S. Covino Jr., B.D. Sartwell and P.B. Needham Jr., J. Electrochem. Soc. 125 (1978) 366.
[11] V. Ashworth, D. Baxter, W.A. Grant and R.P.M. Procter, Corr. Sci. 16 (1976) 775.